RESEARCH PAPER

High Temperature Tensile Behavior of A356 -TiB_2/ TiC In-Situ Composites

I. Kakaravada[1], A. Mahamani[2*] and V. Pandurangadu[1]

** mahamanisudhan@gmail.com*

Received: May 2019 **Revised: September 2019** **Accepted: November 2019**

[1] Department of Mechanical Engineering, Jawaharlal Nehru Technological University, Anantapuramu, Andhra Pradesh, India.

[2] Department of Mechanical Engineering, Sri Venkateswara College of Engineering &Technology (Autonomous), Chittoor, Andhra Pradesh, India.

DOI: 10.22068/ijmse.17.1.56

Abstract: *In the present investigation, A356-TiB_2/TiC composites with a various reinforcement ratios (0, 2.5, 5 and 7.5%) were synthesized through a K_2TiF_6-KBF_4-Graphite (C) reaction system. Formation of TiB_2 and TiC particulates and their distribution are confirmed by various characterization techniques. The tensile properties such as ultimate strength, yield strength, young's modulus and percentage of elongation in addition to their failure behavior of were studied at ambiant and high temperatures (100, 200 and 300^{0}C). The increment in the volume fraction of the composite raised the hardness and the enhancement of hardness was reported up to 49% at 7.5% reinforced composite due to the strengthening effect. The density and porosity of fabricated composites were investigated. The rise in the volume fraction of reinforcement phase decreased the density and increased the porosity of composite samples. Further, the ultimate strength, yield strength, young's modulus declined with the rise in the temperature. Result analysis also illustrates that the 7.5% reinforced composite retained the ultimate strength up to 84.4% and the ductility was raised by 27% at 300^{0}C. Yield strength and young's modulus were also retained 74.31% and 71.09% respectively at the similar material and experimental conditions. The fracture surface analysis of the composites showed that, the ductile nature of failure appearance microscopically with the formation of fine dimples and voids on fracture surface at elevated temperatures. Cleavage facets and tear crumples observation indicated the brittle kind of failure at the ambient temperature. Findings from the experimental study provide the tensile behavior of the composites at the regular working temperature of the automobile engine piston.*

Keywords: *A356-TiB_2/TiC In-situ composites, Stir casting, Mechanical properties, Fractrographic analysis.*

1. INTRODUCTION

Utilization of aluminum metal matrix composites (AMMCs) has been growing due to their superior properties like strength to load ratio, greater specific stiffness, extreme wear resistance, lesser density, good thermal conductivity, supreme electrical conductivity and lower thermal expansion coefficient [1]. The aforesaid reason authenticates to make use of AMMCs at countless engineering applications in space, automotive and aerospace industries. [2-3]. The particulate reinforced composite exhibits extreme mechanical property, heat bearing ability and oxidation resistance as compared with as fiber or whisker reinforced composites [4]. Aluminum matrix composites are produced by ex-situ and in-situ techniques. In ex-situ technique, the composites are produced by mixing the reinforcement into a hot molten matrix. Formation of aggravation of reinforcements in a particular region and poor adhesion between the reinforcement and matrix interface is notable limitations of the ex-situ composites which causes a decline in the load-bearing ability and mechanical properties [5]. The fabrication method for in-situ composite has numerous advantages such as smaller size particle formation with oxide-free and dirt free, thermodynamic stability and homogeneous dispersion of particle in the matrix. The aluminothermic reaction during fabrication facilitates the wetting between the matrix and reinforcement. The evenly distributed reinforcement particles in the matrix, in this technique, raises the mechanical and wear properties of composites [6]. TiB_2 and TiC ceramics have greater hardness, tremendous stiffness and are good toughening and the strengthening agent when adding with aluminum [7-8]. A356 alloy is unavoidable ma-

[DOI: 10.22068/ijmse.17.1.56]

terial in automotive industries due to its superior load-bearing ability, resistance to corrosion and castability. However, the formation of dendritic acicular silicon eutectic along with α-Al during casting process dilutes the mechanical properties of the composite [9]. The addition of TiB_2 and TiC ceramics restrict the dendrite formation and refine the aluminum grains. Synthesis and evaluation of mechanical properties of the in-situ composites are widely discussed in the literature. Kumar et al. [10] studied the influence of TiB_2 particulates into the Al-7Si aluminum matrix and noted a considerable hike in mechanical properties of the composites due to the grain refinement of α- aluminum with modification of eutectic phase of silicon content. Dinaharan et al. [11] produced the ZrB_2 reinforced composites by the using Al-K_2ZrF_6-KBF_4 reaction system. Their investigation result disclosed that the UTS and hardness of composites were enhanced due to the addition of ZrB_2 and also found that the increment in volume content of ZrB_2 raised the mechanical properties. Lijay et al. [12] synthesized the Al-TiC composite by reacting Al-K_2ZrF_6-SiC system. They observed the TiC formation with hexagonal, cubic and spherical shapes. The aforesaid TiC particulates and their uniform distribution raised the ultimate tensile strength and micro hardness. Nevertheless, the mechanical properties like hardness, yield strength, tensile strength and ductility of the material are strongly reliant on the microstructure and these properties will be variable when the environment changes during the real-time application. In this unique situation, the knowledge on the mechanical properties at room temperature is not adequate to predict the reliability of the material at the service conditions [13]. Bhagat et al. [14] reported that more than 114% enhancement of tensile strength of the AA6061-SiC whisker reinforced composites over the unreinforced alloy at room temperature. Further, the strength of the composite was 60% more than the AA6061 alloy at 350°C. Kumar et al. [15] described the high-temperature strength and strain hardening behavior of the AA5052-9% ZrB_2 in-situ composites. The strength of the composite was retained about 81% at 150 ^{0}C whereas the strength was declined into 72% at 200 ^{0}C. Oñoro [16] presented a comparative study of mechanical properties of AA6061-TiB_2 and AA7015-TiB_2 composites at elevated temperatures. It was found from the results, that the AA7015-TiB_2 composites have greater strength than the AA6061-TiB_2 at room temperature, 100^{0}C and 200^{0}C. However, the reduction in strength was in faster rate after 200^{0}C in both composites and the strength of both composites was equal at 500^{0}C. Han et al. [17] noted the significant raise in the modulus of elasticity of the Al-Si/TiB_2 composite over the unreinforced alloy at the temperature range of 25–350^{0}C. The comparative study illustrates that the greater yield and tensile strength than unreinforced alloy at room temperature. However, there is no significant increase in the yield and tensile strength when compared to the unreinforced alloy at a temperature range of 200 and 350^{0}C. Various automobile components such as pistons, cylinder block, brakes, and brake drums need to be operated at high-temperature conditions during their service. Therefore, assessment of the high-temperature strength of composite material is more essential to predict the service life of aforesaid applications. However, the investigation on high-temperature mechanical properties of the aluminum-based in-situ composite is still deficient and the fracture mechanisms at a greater temperature of this sort of material still have not been completely comprehended. The motivation behind the present investigation is to study the tensile behavior of A356-TiB_2/TiC in-situ composites of different reinforcement ratio under room temperature, 100, 200 and 300^{0}C which are the regular working temperature of the automobile engine piston. The mechanism of failure under tensile load also described through fractrographic analysis.

2. EXPERIMENTAL DETAILS

2.1. Materials and Fabrication Method

In the present investigation, A356 alloy was chosen as a matrix material. The chemical constituent presented in A356 alloy is Si-6.5%, Fe-0.15%, Cu-0.03%, Mn-0.10%, Mg-0.4%, Zn-0.07%, Ni-0.05 and Ti-0.1%. The composite materials were prepared by reacting of the aluminum melt with halide salts namely, potassium hexa flurotitanate (K_2TiF_6), potassium hexa-fluroborate (KBF_4) and

[DOI: 10.22068/ijmse.17.1.56]

graphite (C). Composite materials were prepared with various weights percentage of reinforcement from 0 to 7.5% with an increase in a step of 2.5% by varying the salt quantity. The quantity of the halide salts and graphite for fabricating each composite sample is illustrated in the Table 1. Initially, the A356 aluminum alloy ingots are heated up to 850ºC in the electric bottom pouring stir casting furnace and measured quantity of preheated halide salts were added to the aluminum melt". The schematic layout of the stir casting setup is illustrated in Fig.1. The aluminum melt starts reactions with these salts and facilitates an aluminothermic reaction. This aluminothermic reaction produces massive temperature up to 1200^{0}C (exothermic) in Aluminum melts and facilitates the reaction between aluminum, halide salts and graphite and originates the formation of TiB_2 and TiC reinforcement particulates.

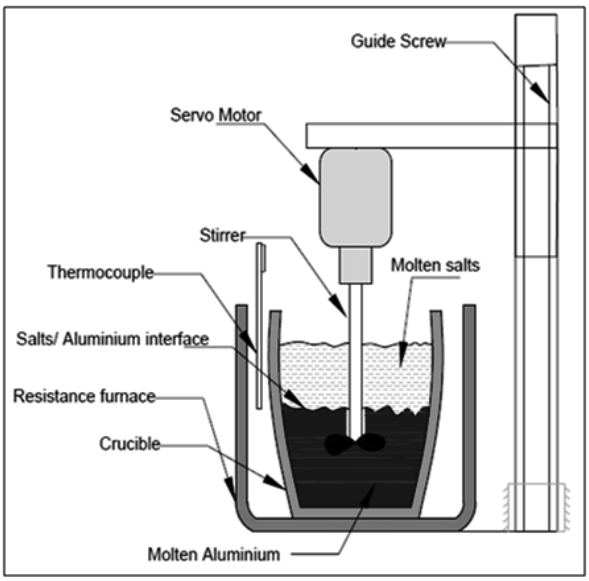

Fig. 1. Schematic layout of stir casting furnace

On the other side, this reaction promotes automatic boiling and stirring effect in the melt which causes homogeneous dispersion reinforcement particles in the melt. Further, the melt was stimulated by stirrer intermittently to attain uniform dispersion of reinforcement. The aluminothermic reaction results in the formation of residue products like $KAlF_4$ (potassium aluminum fluoride) and K_3AlF_6 (potassium fluro aluminate) within the melt. These residues must be evacuated from the melt before pouring into the cavity to make the defect-free casting. Now the residue-free TiB_2 and TiC reinforcements are generated within the aluminum melt. Further it was poured into preheated (300ºC) metallic die with a dimension of 150×150×15 mm and allowed it to cool. The fabricated A356-TiB_2/TiC composites are separated from the mold cavity and used for further investigations.

2.2. Characterization of Composite Samples

Initially, the fabricated composites were characterized through computerized metallurgical microscope fixture with an advanced digital camera (Model: Metzer-VFM9100). First, composite specimens were taken in the required dimensions from the fabricated composite plate and polished with various grades of alumina sheets followed by disk polishing until the specimen surface was free from scratches. The smooth surface specimen etched for 10 seconds with Keller solution which has 1.5% HCL, 2.5% HNO_3, 1% HF and 95% H_2O. The etched specimens were used to capture the optical micrographs. From the captured images the grain length of the composite was measured through micro cam software (version 4.0). The various grain lengths are measured from the captured images and the average value grain size was reported. The microstructure of fabricated com-

Table 1. Quantity of salts were added for the fabrication of composites

Composite	A356 alloy(g)	K_2TiF_6(g)	KBF_4(g)	Graphite(g)
A356 alloy	1000	Nil	Nil	Nil
A356-2.5% TiB_2/TiC	917	30	35	18
A356-5% TiB_2/TiC	845	60	70	25
A356-7.5% TiB_2/TiC	775	90	105	30

[DOI: 10.22068/ijmse.17.1.56]

posites was captured by using a scanning electron microscope (Model: JOEL-6360LV). This microstructure disclosed the uniform dispersion and wettability of the reinforcement phase within the matrix material. Further, the EDAX spectra of A356-7.5% TiB_2/TiC was captured by using the energy dispersive X-Ray (Hitachi S-300 H a model) lithium drift silicon analyzer with a working voltage 20 kV to record the pattern to investigate the chemical constituent presents in the fabricated composite. The phase analysis of A356-TiB_2/TiC composites was investigated through X-ray diffractometer (Model: XPERT-Pro) employing Cu-kα radiation with generator parameters of current 30mA and 40kV with a continuous scanning speed of 1^0/min. The generated XRD spectrums validate the chemical compounds and formation of the reinforcement phase in the composite through an aluminothermic reaction.

2.3. Evaluation of Physical and Mechanical Properties.

The fabricated composites have undergone various mechanical property investigations like micro hardness, density, porosity and tensile properties like ultimate tensile strength, yield strength, % of elongation and young's modulus were evaluated at room and elevated temperature. The micro Vickers hardness assessment of A356-TiB_2/TiC composites was carried out utilizing micro Vickers hardness tester with one-kilogram load for a minimum operating dwell time of 8 seconds at least three distinctive locations were recorded. The average values of reading were reported. The relative density of composites was measured by employing the Archimedes principle. In this method, the aluminum composites sample simply weighed in atmospheric air and distilled water by using a density measurement kit (Model: AD-1653) and weights are recorded. The equation 1 was used to calculate the relative density for the composite samples.

$$\text{Relative density} = \frac{W_{air}}{W_{air} - W_{water}} \quad (1)$$

where W_{air} = weight of composite sample in air, W_{water} = weight of composite sample in purified water. Using this equation (1), the base alloy and composite materials relative densities were evaluated. During the casting processes of composite samples, some extent of porosity is acceptable because of the long particle supply to the liquid melt and rise in surface area in contact with air. The volume fraction pore content in casted composites plays a crucial role in the mechanical behavior of composites this reason validates the porosity levels in fabricated composite must be kept a minimum. However, the porosity cannot be avoided but it can be controlled. The porosity of composites material was calculated by the following equation

$$Porosity = \frac{\rho_{th} - \rho_m}{\rho_{th}} \quad (2)$$

where ρ_{th} and ρ_m are the theoretical and measured densities of composite material respectively. The theoretical density of composite material was calculated through the rule of a mixture according to their availability of chemical constituent present in the composite material. The mechanical behavior of A356-TiB_2/TiC composites was evaluated under ambient and elevated temperature on the computerized universal testing machine (Servo Electric Hot forming Machine, Electra-50) with maximum loading facility of 50 kN and the specimen heating capacity of 1000^0C. The specimen prepared for the test as per the dimensions of ASTME8/E8M-11 standard form the casted plates and placed in the fixture which is surrounded with split type furnace. The specimen is heated to the required testing temperature at a heat-up rate of 20^0 C/min up to necessary testing temperature. The heat conservation time of specimen is 5–10 minutes to make sure that an identical temperature has reached before loading on the sample. The tensile test has been conducted at a fixed strain rate of 0.0001 S^{-1} with altered temperatures from room temperature to 300^0C for all the composite samples. High temperature contact type extensometer was used for analyzing strain behavior of specimen at lofty temperatures during the test. The stress-strain data from the universal testing machine is used to analyze the tensile characteristics of composites at various temperature conditions. The specimen prepared for the test as per the dimensions of ASTME8/E8M-11 standard form the casted plates and placed in the fixture which is sur-

[DOI: 10.22068/ijmse.17.1.56]

rounded with split type furnace. The specimen is heated to the required testing temperature at a heat-up rate of 20^0C/min up to necessary testing temperature. The heat conservation time of specimen is 5–10 minutes to make sure that an identical temperature has reached before loading on the sample. The tensile test has been conducted at a fixed strain rate of 0.0001 S^{-1} with altered temperatures from room temperature to 300^0C for all the composite samples. High temperature contact type extensometer was used for analyzing strain behavior of specimen at lofty temperatures during the test. The stress-strain data from the universal testing machine is used to analyze the tensile characteristics of composites at various temperature conditions.

3. RESULTS AND DISCUSSIONS

3.1. Optical Microscopic Characterization

The optical photo image of A356 alloy is shown in Fig. 2(a). From Fig. 2(a), one can observe the formation of a secondary dendrite structure with a modified eutectic phase of silicon in A356 alloy. The distinctive dendrite structure was observed in cast alloy because of α-aluminum dendrites are stretched out with a greater aspect ratio due to the rapid cooling rate of the alloy during the solidification processes. Fig. 2(b)-(d) represent the photomicrograph of A356 alloy composites with a various volume fraction of TiB_2/TiC reinforcement. From Fig. 2(b)-(d), it is observed that the refinement of α-aluminum grains occurs due to the presence of TiB_2 and TiC reinforcement particles. The generated reinforcement particulates act as nucleus points and thereby control the size of α- aluminum grains during the solidification. This mechanism enhances the formation of fine grains during the solidification processes. A variety of size and shape of TiB_2 and TiC particulates generated through K_2TiF_6-KBF_4-Graphite (C) reaction system which is uniformly distributed all over the matrix. The generated particulates of TiB_2 particulates are in hexagonal [25] and TiC simple cubic in shape [26] respectively as shown in Fig. 2(b) and (C). The in-situ generated particles are up to micron, submicron and nanoscales. The cluster formation of par-

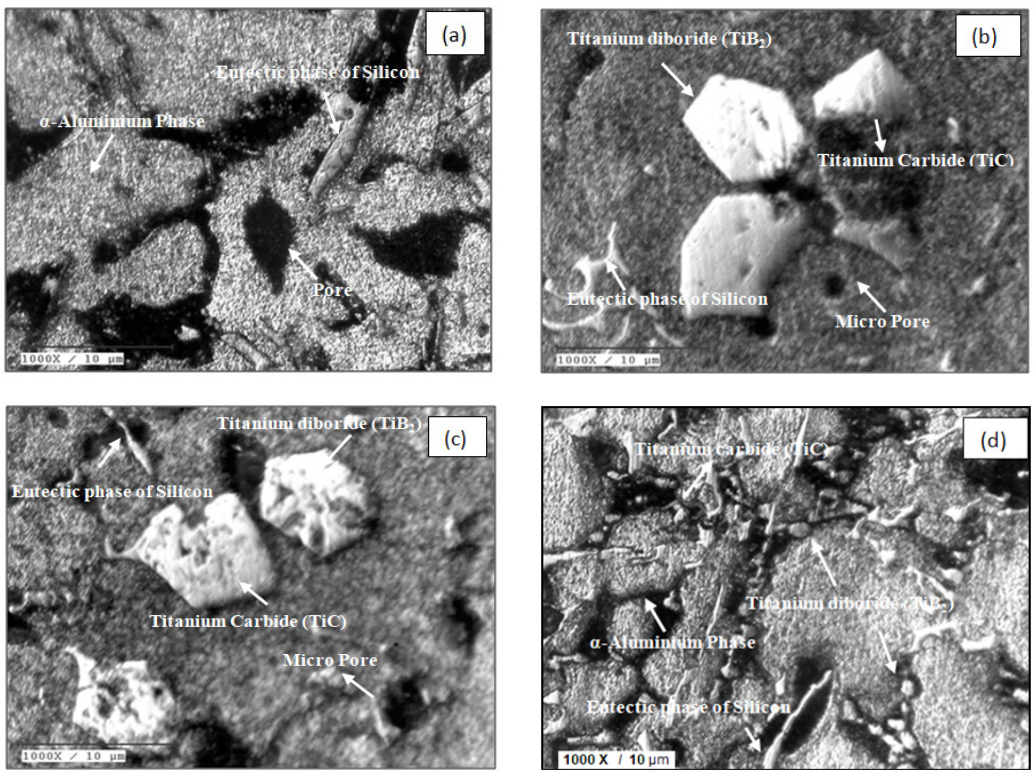

Fig. 2. Optical micro graphs of A356-TiB_2/TiC composite (a) A356 alloy (b) A356-2.5% TiB_2/TiC (c) A356-5% TiB_2/TiC (d) A356-7.5% TiB_2/TiC

[DOI: 10.22068/ijmse.17.1.56]

ticles depends on the reaction temperature, holding time and rate of cooling [20]. The wettability effect between particulates and melt hold up the movement of the TiB_2/TiC particles and it can uniformly disperse in the melt for a long time. During the solidification processes α-aluminum crystallize as a primary phase simultaneously the TiB_2 and TiC particles are moved to the solidification interface which is displayed in Fig. 2(d). .From Fig. 2(d) it is also observed that the TiB_2 and TiC particulates are well bonded with A356 matrix. The alumino-thermic reaction promotes a rise in local temperature which enhances the wettability effect between the particle and matrix material. There are no voids and reaction products are surrounded by the particulates which indicate excellent interfacial bonding between reinforcement and matrix.

3.2. Scanning Electron Microscope and Energy Dispersive X-Ray Analysis

Fig. 3(a)-(d) illustrates the scanning electron photomicrograph of composite samples with a distinct reinforcement ratio. The existence of TiB_2 and TiC reinforcement in the matrix and their distribution are exposed in Fig. 3(a)-(d). The clean interface between the matrix and reinforcement, clear and clutter-free and homogenously distributed reinforcements throughout the matrix are found in Figs. 3(a)-(d). Fig. 3(e) shows the energy dispersive X-Ray pattern of A356-7.5% TiB_2/TiC composite. The formations of TiB_2, TiC, and other alloying elements are detected in the spectrum and no other impurities or intermediate compounds are detected

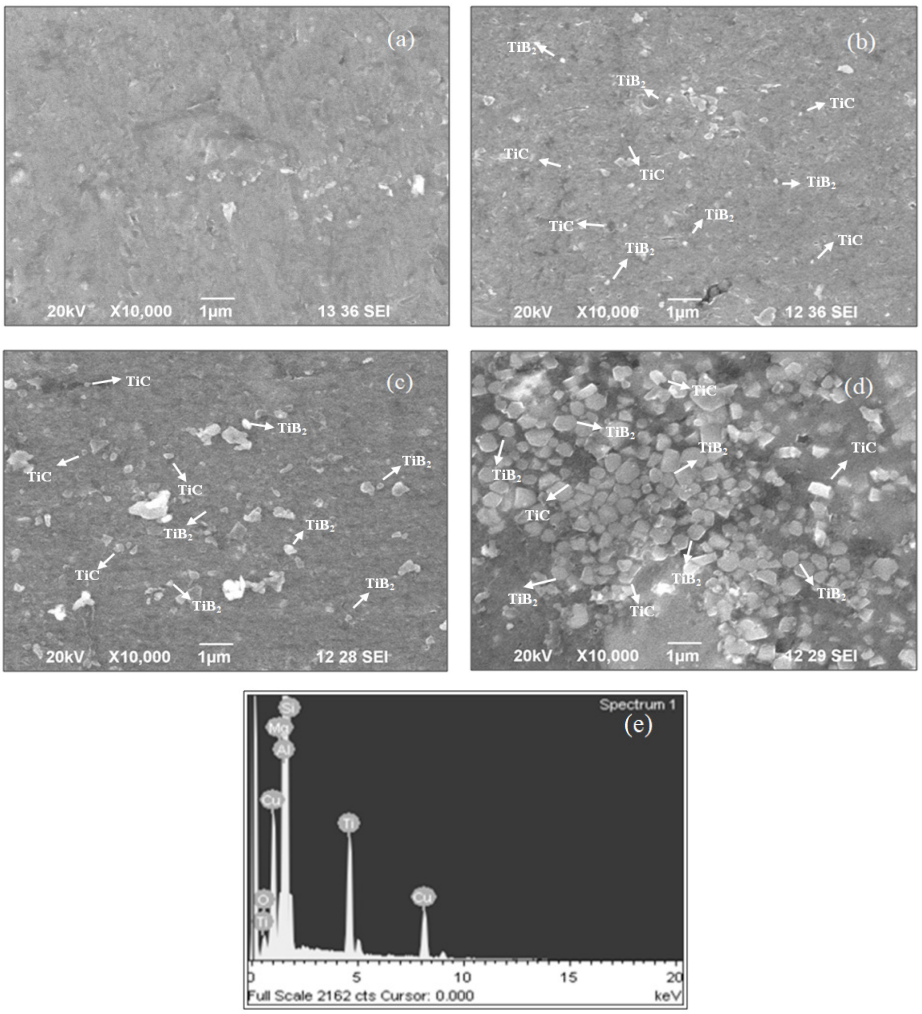

Fig. 3. Scanning electron micrographs of A356-TiB_2/TiC composites (a) A356 alloy. (b) A356-2.5% TiB_2/TiC. (c) A356-5% TiB_2/TiC. (d) A356-7.5% TiB_2/TiC. (e) EDAX spectra A357.5%TiB_2/TiC composite.

[DOI: 10.22068/ijmse.17.1.56]

3.3. Phase Analysis of A356-TiB_2/TiC In-Situ Composites

The generated X-ray diffraction analysis (XRD) patterns of in-situ A356-TiB_2/TiC composites are depicted in Fig. 4. The TiB_2 and TiC ceramic reinforcement phase were generated through an aluminothermic reaction. The various stages of reactions taking place in the aluminum melt at 850^0 C is given by following equations:

$$3K_2TiF_6+13Al \rightarrow 3Al_3Ti+3KAlF_4+K_3AlF_6 \quad (1)$$
$$2KBF_4+6Al \rightarrow 4AlB_2+2KAlF_4 \quad (2)$$
$$Al_3Ti+AlB_2 \rightarrow TiB_2+4Al \quad (3)$$
$$3K_2TiF_6+4Al \rightarrow 3\,Ti+3KAlF_4+K3AlF_6 \quad (4)$$
$$Ti+3Al \rightarrow Al_3Ti \quad (5)$$
$$Al_3Ti+C \rightarrow TiC+3Al \quad (6)$$

The above reaction leads to the formation of cryolite residues like $KAlF_4$ and K_3AlF_6 which were removed from the melt.

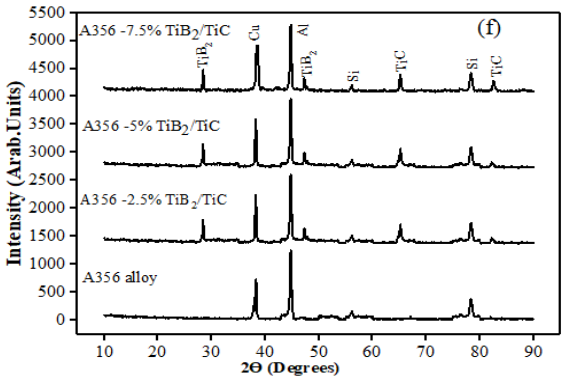

Fig. 4. XRD spectra of A356-TiB_2/TiC in-situ composite

The peaks in the pattern of A356 monolithic alloy and A356-2.5 to 7.5% TiB_2/TiC confirms the presence of aluminum and reinforcement particulates. Peaks of A356 matrix material were observed at 39.50, 45.10, 56.50 and 83.50 degrees with plane indices <1, 1, 1> respectively as well peaks corresponding of TiB_2 and TiC observed at 29.50, 48.60, 66.80 and 79.5 degrees with plane indices <0, 0, 2 >. It is clear from the spectrum that the successful formation of TiB_2 and TiC particulates were generated through aluminothermic reaction. Further, it is also stated that no impurities or intermetallic compounds were observed in the casted composite.

3.4. Grain Size Measurement and Micro Hardness

The grain size in the fabricated sample is the most influencing parameter on the mechanical behavior of composites material. The fine grains structure in fabricated composite material exhibits superior mechanical and wear properties. In the present work, the effect of an increase in the reinforcement phase in aluminum melt on the grain size of composites was investigated. The measured grain size values are depicted in Fig. 5. It is evident from Fig. 5, that an increase in reinforcement ratio declines the grain size. The TiB_2 and TiC particles obstruct the solute redistribution and refine eutectic silicon. This mechanism leads to the dendrites of α- aluminum to convert to a fine equiaxed grain structure in fabricated composites [10]. It can be noted from Fig. 5, the micro Vickers hardness of A356-TiB_2/TiC composites is raised by increasing the reinforcement ratio. More than 11%, 35 % and 49 % enhancement in hardness over the A356 alloy are observed at 2.5%, 5% and 7.5% reinforced composites respectively. The increment in reinforcement causes grain refinement and controls the flow of dislocation in the matrix. This mechanism restricts the penetration of indenter on the surface of composites and leads to an increase in the hardness of composites. Further, the presence of TiB_2 and TiC particulates tends to strengthen the composites due to their mismatch of coefficient of thermal expansion. This mechanism develops the mismatch strains at the interface of reinforced particulates and A356 matrix and hinders the dislocation movement in turn increase hardness of composites [18].

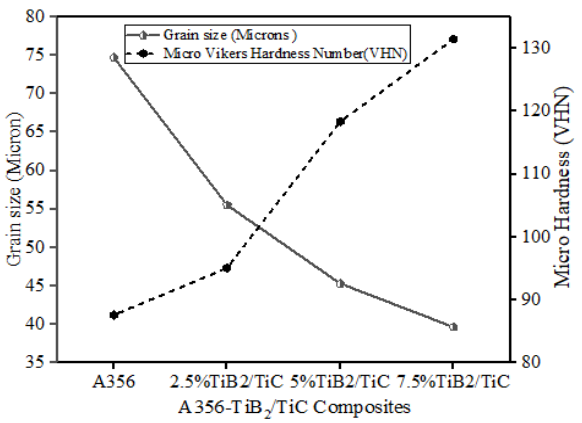

Fig. 5. Grain size and Hardness of composites.

[DOI: 10.22068/ijmse.17.1.56]

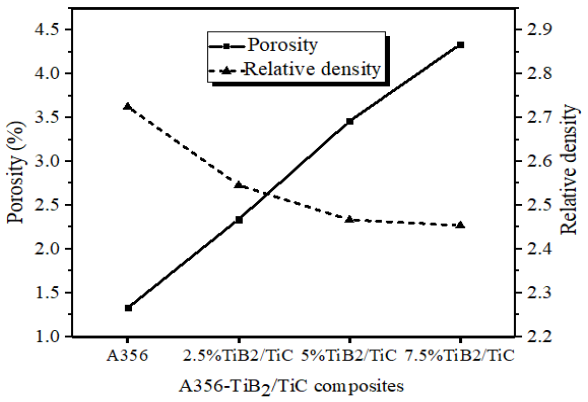

Fig. 6. Porosity and Relative density of composite

3.5. Density and Porosity Measurement

Fig. 6 depicts the differences in the measured density of A356 aluminum alloy and A356-TiB_2/TiC composite material. From Fig. 6, it is observed that the density of composite samples diminishe with the increase in reinforcement phase. The density of A356-TiB_2/TiC composites is less as compared to the A356 alloy due to the presence of TiB_2 and TiC particulates. Porosity content of A356 aluminum alloy and its composites are calculated through equation 2 which is depicted in Fig. 6. The porosity of A356 alloy is less as compared with the A356-TiB_2/TiC in-situ composite material. The increase in volume fraction of reinforcement particulates is attributed to increase in porosity content in fabricated composites due to gases entrapment and shrinkage of matrix material during the solidification processes. [24].

3.6. Evaluation of Tensile Properties

The ultimate tensile strength (UTS), yield strength (YS) and percentage of elongation (EL) were investigated for various composite materials and are illustrated in Fig. 7-10. Fig. 7 depicts that the ultimate strength of composites is more than the A356 alloy for all tested condition. It is also evident from Fig. 7, the increment in reinforcement ratio enhanced the UTS of the composites. The presence of smaller size TiB_2 and TiC particulates and smaller grains of metal matrix acted as a load-bearing element and controlled the flow of tensile stress to the matrix material due to superior interfacial bond strength derived from the aluminothermic reaction. Further, the fine particulate minimizes the void formation and stress concentration at grain boundaries under the tensile loading condition which maximizes the strength of composites. The differences in the coefficient of thermal expansion between matrix and reinforcement particulates influence the strengthening mechanism of a composite. This variation makes possible to a greater concentration of dislocations in the region of the reinforcement particulates during solidification. The availability of appending dislocation around the TiB_2 and TiC particulates and the variation in the thermal expansion coefficient of particulate and matrix contributes to the enhancement of the ultimate tensile strength of composites [17]. The increase in test temperature of the specimen from ambient to 300^{0}C, causes the ultimate strength of A356 alloy and its composites reduce significantly. More than 91.2 % retainment of UTS at 100^{0}C, 88.2 % retainment of UTS at 200^{0}C and 84.4 % of UTS at 300^{0}C was observed for the 7.5 % reinforced composites. It is also evident from Fig. 7; the increment in TiB_2/TiC contents improves the UTS of composites at elevated temperature.

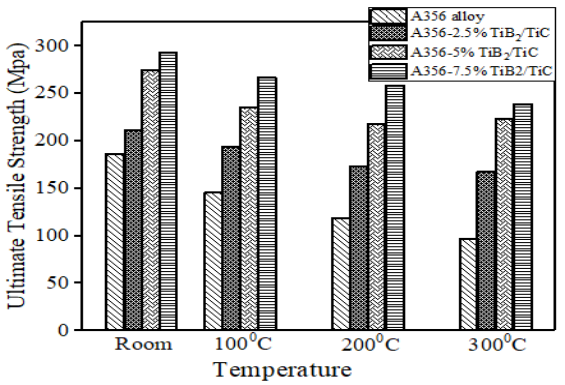

Fig. 7. Influence of temperature on UTS of composite

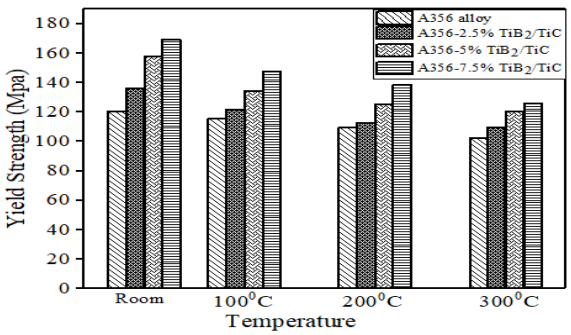

Fig. 8. Influence of temperature YS composites.

[DOI: 10.22068/ijmse.17.1.56]

Fig. 8 demonstrates that, the yield strength (YS) of A356-TiB_2/TiC composites at room and elevated temperature at a constant strain rate of 0.0001 S^{-1}. The yield strength of composites is greatly enhanced with an increase in reinforcement ratio for all tested conditions. The considerable improvement in YS of the composite is recorded with the integration of TiB_2 and TiC reinforcement into the matrix. These fine reinforcement particulates act as nucleation sights during the solidification processes which results in the formation of equiaxed fine grains. The refinement of grains will restrict the stress flow and accumulation of dislocation under the tensile loading condition. This mechanism enhances the YS of composites [19]. However, an increase in TiB_2/TiC particulates improves the YS of composites at elevated temperatures. Further, 83.1 % retainment of YS at 100^{0}C, 81.6% retainment of YS at 200^{0}C and 74.3 % of YS at 300^{0}C are noted for the 7.5 % reinforced composites. At greater temperature causes the fewer impact of strain hardening exponent component. The enhancement in strain hardening capacity of a composite at elevated temperature leads to minimum variations in yield strength of composites [15].

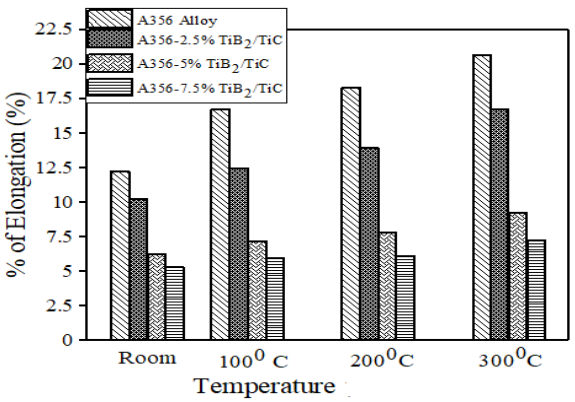

Fig. 9. Influence of temperature on elongation

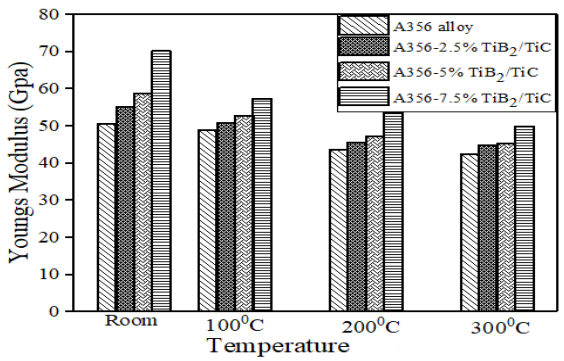

Fig. 10. Influence of temperature on youngs modulus

Fig. 9 exemplifies that, the effect of temperature on the percentage of elongation of A356-TiB_2/TiC composite at room and high temperatures at a strain rate of 0.0001 S^{-1}. An increase in reinforcement ratio reduces the percentage elongation of composites when compared with the A356 alloy for all tested condition. It is evident from Fig. 9; that the increase in reinforcement shortens the ductile matrix phase in the fabricated composites. The presence of TiB_2 and TiC particulates facilitates Orowin loop formation around the particulates. This loop controls the deformation of grain boundaries under applied tensile load and declines the elongation of composites [21]. It is also noted from Fig. 9, the elongation of composite material is increased by increasing the temperatures. More than 12 % increment of elongation at 100^{0}C, 16 % increment of elongation at 200^{0}C and 27 % increment of elongation at 300^{0}C are observed for the 7.5 % reinforced composites. The fine grain formation directed to the uniform distribution of deformation stresses under the tensile loading condition which leads to recovered plasticity of the material. This mechanism directs to enhance the elongation of material at high temperature [22]. Fig. 10 depicts the effect of temperature on the Young's modulus of A356-TiB_2/TiC composites at room and elevated temperatures at the strain rate of 0.0001 S^{-1}. The Young's modulus of composite material is greater than the A356 alloy for all tested conditions and further increases with an increase reinforcement ratio. The presence of TiB_2 and TiC reinforcement enhances the Young's modulus of the composite under tensile loading through the effective transformation of the applied tensile load from the matrix to reinforcement. The strong interfacial bond strength between the particulates encouraged with the nucleation of α-aluminum on the TiB_2 and TiC particulates and efficient load transfer thereby maximize the Young's modulus improvement [23]. It can also be seen from Fig. 10, that the rise in temperature declines the Young's modulus of composites. Further, 81.7 % retainment of Young's modulus at 100^{0}C, 76.2 % retainment of Young's modulus at 200^{0}C and 71.3 % of Young's modulus at 300^{0}C is noted for the 7.5 % reinforced composites. It is due to the softening of matrix laterally with the plastic flow along the perpendicular direction of the applied load. This mechanism facilitates the moving of dislocations within the ma-

[DOI: 10.22068/ijmse.17.1.56]

trix and mechanism is more severe by increasing the temperature and declines the Young's modulus of composites further [16].

3.7. Fracture Surface Analysis

The fracture surface analysis of A356-TiB_2/TiC composites was performed after the tensile test to investigate the failure mechanism and bonding characteristics of reinforced particulates in the composites. The failure mechanism of composites characterized in three different sources namely, interfacial de-cohesion of reinforcement particulates in the matrix, fracture of reinforcement particulates and failure of the matrix material. The variations in fracture surface have exemplified the differences in mechanical properties of the casted composites. Fig. 11 (a) depicts the fractography of A356 aluminum alloy under ambient temperature at a strain rate of 0.0001 S^{-1}. The fracture surface of A356 alloy composed with numerous tearing edges, equiaxed dimples and shear zones under applied tensile load. This kind fracture surface indicates the ductile nature of fracture of A356 alloy at room temperature.

Fig. 11 (b) shows the fracture surface of A356 alloy at 300^{0}C temperature. From Fig. 11 (b), it is observed that the A356 alloy with fine secondary dendrite arm structure exhibited the greater tendency of ductile fracture with fine dimples than the A356 alloy at room temperature with modified eutectic silicon grain size. The fractography of A356-2.5% TiB_2/TiC in situ composites at ambiance temperature is illustrated in Fig. 12 (a). Fig. 12 (a) shows that the existence of TiB_2 and TiC particulates which is non-shearable and which will control the movement of the dislocations under the tensile load. This mechanism creates shallow dimples and microvoids on the fractured surface. Fig.12 (b) illustrates that the micrographs of A356-2.5% TiB_2/TiC at elevated temperature. The surface exhibits various shear face fracture and cleavage surfaces forms through joining of microvoids along with the shear and slip bands which creates a coalescence of dislocation. At elevated temperature, the fracture plane of A356-2.5% TiB_2/TiC composite exhibits a ductile appearance as like of A356 monolithic alloy.

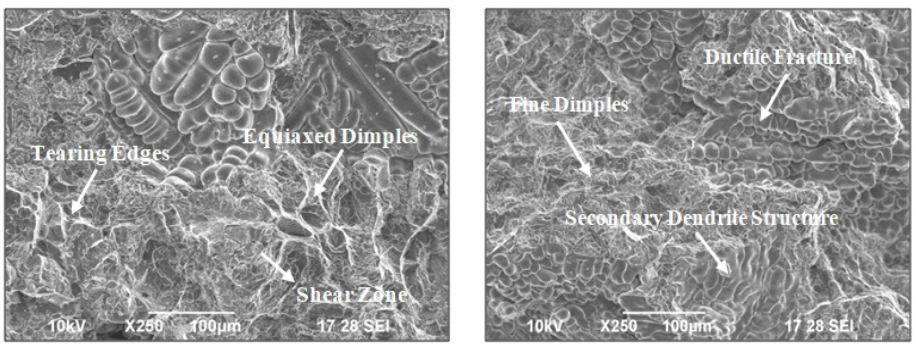

Fig. 11. (a) Fractrography of A356 at room temperature (b) at 300^{0}C temperature.

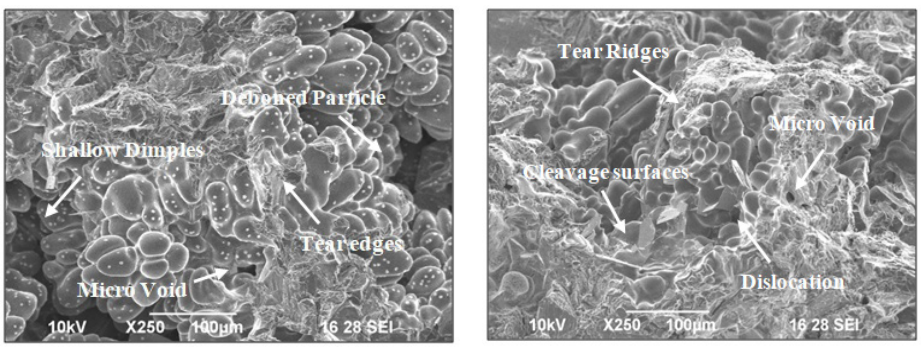

Fig. 12. (a) Fractrography of A356-2.5% TiB_2/TiC at room temperature. (b) at 300^{0}C temperature

[DOI: 10.22068/ijmse.17.1.56]

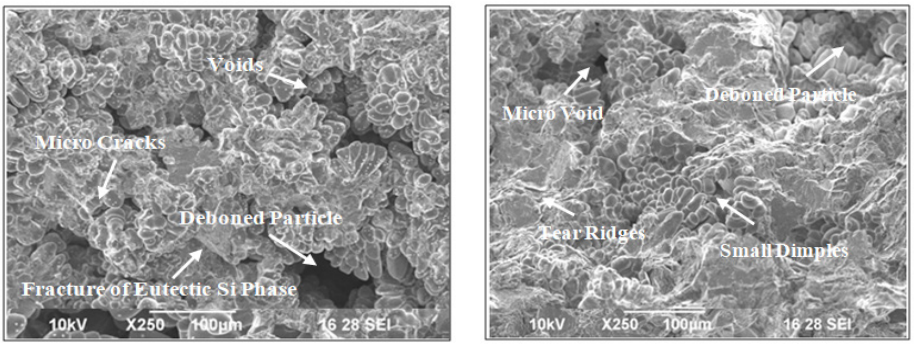

Fig. 13. (a) Fractrography of A356-5% TiB_2/TiC at room temperature. (b) at 300^{0}C temperature.

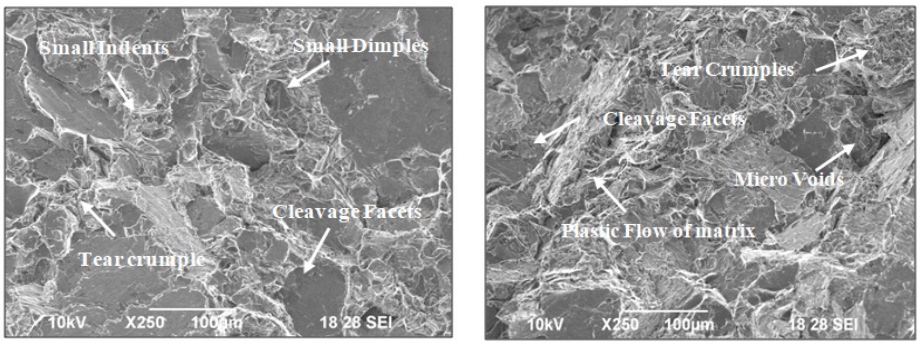

Fig. 14. (a) Fractrography of A356-7.5% TiB_2/TiC at room temperature. (b) at 300^{0}C temperature.

The fractography of A356-5% TiB_2/TiC composite was recorded at ambient temperature at a constant strain rate of 0.0001 S^{-1} as shown in Fig.13 (a). From Fig. 13 (a), it is observed that the well-built and identical distribution of large voids and microcracks were observed on the surface. During the solidification processes of composites, the TiB_2 and TiC particulates are relocated near to the grain boundaries. The main alloying element eutectic silicon phase segregated to intra-dendrite region. This mechanism directed to the generation of microcracks along the grain boundaries. The fracture of eutectic silicon phase and reinforcement particles induce the failure of the specimen under tensile loading condition which implies fracture of specimen mainly caused due to the failure of matrix alloy. Fig. 13(b) illustrates the fracture topology of A356-5%TiB_2/TiC in-situ composites at a higher temperature. Local stress generated by the high temperature is not enough to crash the particulates because of small matrix flow stress. Further, the matrix does not accommodate the generated strain and originates the formation of microvoids and debonding of particulates at the interface. This mechanism shows the way to the formation of tear ridges and small dimples. The fracture topology shows brittle kind of fracture macroscopically and ductile microscopically at elevated temperature. Fig. 14 (a) depicts that the fracture topology of A356- 7.5% TiB_2/TiC in-situ composites at ambiance temperature under the strain rate of 0.0001 S^{-1} The fracture topology illustrates the combination of cleavage facets, tear crumples and small indentations due to the existence of the greater volume fraction of TiB_2/TiC particulates. The formation of cleavage facets was due to the existence of greater intensity of the TiB_2/TiC particles and facilitates the rupture path at an angle to the normal plane. Furthermore, the TiB_2 and TiC particulate from the equiaxed grain and decline the stress concentration around the particulate, in turn, improves the load-bearing ability. Small indentation on the fracture surface was observed due to separated reinforced particulates under the tensile loading condition. This mechanism exhibits the brittle failure of composite material. Fig. 14 (b) depicts that the fracture topology of A356-7.5% TiB_2/TiC in-situ composites at a higher temperature with a predetermined strain rate of 0.0001 S^{-1}. The extensive plastic flow

[DOI: 10.22068/ijmse.17.1.56]

of matrix in the region of the TiB_2/TiC particles can be observed, which exposes the sound interfacial bond between particulates and matrix alloy in addition to the debonding of reinforced particles are detected. Further, the cluster formation of TiB_2 and TiC particulates cannot embark on stress transmission effectively when the material is subjected to a specified load. This mechanism allows the failure in brittle nature which could demise the ductility of the composite. Han et al. [17] also observed a similar behavior in their work.

4. CONCLUSIONS

A356-TiB_2/TiC composites were synthesized through an exothermic reaction of K_2TiF_6-KBF_4-Graphite reaction system:

1. Characterization report illustrates the presence of TiB_2 and TiC particulates, their homogeneous distribution within the matrix and oxide-free interface between the matrix and reinforcements.
2. The increase in volume fraction of reinforcement phase increases the porosity and decreases the density of composites over unreinforced alloy.
3. The increment in the volume fraction of the reinforcement raises the hardness and the enhancement of hardness was reported up to 49 % at 7.5 % reinforced composite over the unreinforced alloy.
4. The ultimate strength, yield strength, Young's modulus declined by raising the temperature. Result of the study illustrates that the 7.5 % reinforced composite retained the ultimate strength up to 84.4 % and the ductility was raised by 27 % at 300^0 C.
5. Yield strength and Young's modulus were also retained 74.31% and 71.09 % respectively at the similar material and experimental conditions.
6. The fractrographic analysis of the composites illustrates that, the ductile nature of failure appearance microscopically with the formation of fine dimples and voids on fracture surface at elevated temperatures.
7. At room temperature, the fractography exhibits numerous cleavage facets and tear crumples were observed due to no shearable property of reinforcement which controls the deformation of the matrix at ambient temperature. This mechanism indicates a brittle kind of failure in composites at ambient temperature.

REFERENCES

1. Parveen, A., Chauhan, R. M. and Suhaib, M., "Study of Si_3N_4 reinforcement on the morphological and tribe- mechanical behaviour of aluminium matrix composites". Mater. Res. Exp., 2019, https://doi.org/10.1088/2053-1591/aaf8d8.
2. Radhika, N. and Raghu, R., "Prediction of mechanical properties and modeling on sliding wear behaviour of LM25/TiC composites using response surface methodology". J. Partic. Sci. Technol., 2016, 36, 104-111.
3. Mahesh Kumar, V. and Venkatesh, C. V., "A comprehensive review on material selection, processing, characterization and applications of aluminium metal matrix composites". Mater. Res. Exp., 2019, https://doi.org/10.1088/2053-1591/ab0ee3
4. Tuo, Xu., Guirong, Li., Menglei, Xie., Ming, Liu., De, Zhang., Yutao, Zhao., Gang, Chen. and Xuzhou, K., "Micro structure and mechanical properties of in-situ nano g - Al_2O_3/A356 aluminium composite". J. alloy. Compo. 2019, 787, 72-85.
5. Tham, L. M., Gupta, M. and Cheng, L., "Effect of limited matrix-reinforcement interfacial reaction on enhancing the mechanical properties of aluminium–silicon carbide composites". Acta Mater., 2001, 49, 3243–3253.
6. Tjong, S. C. and Ma, Z. Y., "Micro structural and mechanical characteristics of in-situ metal matrix composites". Mater. Sci. Eng., 2000, 29, 49–113
7. Yu-jin, W., Hua-xin, P., Feng, Y. E. and Yu, Z., "Effect of TiB_2 content on microstructure and mechanical properties of in-situ fabricated TiB_2/B_4C composites". Trans. Nonferrous Met. Soc. China., 2011, 21, 369-373.
8. Ramaswamy, A., Perumal, A. V. and Chelladurai, S. J. S., "Investigation on mechanical properties and dry sliding wear characterization of stir cast LM13 aluminium alloy- ZrB_2-TiC Particulate hybrid composites". Mater. Res. Exp., 2019, https://doi.org/10.1088/2053-1591/ab0ef8.
9. Zulfia, A. and Putriana, L. T., "Effect of strontium on the microstructure and mechanical properties of aluminium ADC12/Nano-SiC Com-

[DOI: 10.22068/ijmse.17.1.56]

posite with Al-5TiB grain refiner by stir casting method". Mater. Res. Exp., 2019, https://doi.org/10.1088/2053- 1591/ab0a49.
10. Kumar, S., Chakraborty, M., Subramanya Sarma, V. and Murty, B. S., "Tensile and wear behavior of In-situ al-7Si/TiB_2 particulate composite". Wear., 2008, 265, 134-142.
11. Dinaharan, I., Murugan, N. and Parameswaran, S., "Influence of in situ formed ZrB_2 particles on microstructure and mechanical properties of AA6061 metal matrix composites". Mater. Sci. Engg- A., 2011, 528, 5733–5740.
12. Lijay, K., Selvam, J. D. R., Dinaharan, I. and Vijay, S. J., "Microstructure and mechanical properties characterization of AA6061/TiC aluminium matrix composites synthesized by in situ reaction of silicon carbide and potassium flurotitanate. Trans". Nonferrous Met. Soc. China., 2016, 26, 1791-1800.
13. Maisonnette, D., Bardel, D., Robin, V. D. Nelias, D. and Suery, M., Mechanical behavior at high temperature as induced during welding of a 6xxx series aluminium alloy. Int. J. Pressu. Vess., 2017, 149, 55-65.
14. Bhagat, R. B., Amateau, F. M., House, M. B., Meinert, K. C. and Nisson, P., "Elevated Temperature Strength, Aging Response and Creep of Aluminium Matrix Composites". J. Comp. Mater., 1992, 26, 1578-1593.
15. Kumar, N., Gautam, G., Mohan, A. and Mohan, S., "High temperature tensile and strain hardening behavior of AA5052/9 Vol% ZrB_2 in-situ composites". Mater. Res., 2018, 21, 1-7.
16. Onoro, J., "High temperature mechanical properties of aluminium alloys reinforced with titanium diboride (TiB_2) particles". Rare Metals., 30, 2011, 200-205.
17. Han, G., Zhang, W., Zhang, G., Feng, Z. and Wang, Y., "High temperature mechanical properties and fracture mechanisms of Al-Si piston alloy reinforced with in situ TiB_2 particles". Mater. Sci. Engg., 2015, 630, 161-168.
18. Kannan, C. and Ramanujam, R., "Mechanical and tribological behavior of molten salt processed self lubricated aluminium composite under different treatment". Mater. Res. Exp., 2018, 5, 1-14.
19. Bhargavi, R. and Ramanaiah, N., "Investigation on mechanical behavior of B_4C and MsO_2 reinforced AA2024 hybrid composites". J. Manuf. Sci. Prod., 2015, 15, 339-343.
20. Wang, X., Jha, A. and Brydson, R., "In-situ fabrication of Al3Ti particle reinforced aluminum alloy metal-matrix composites". Mater. Sci. Engg-A, 2004, 364, 339-345.
21. Selvam, J. D. R., Dinnaharan, I., Philip, S., and Mashinini, V., "Microstructure and mechanical characterization of in-situ synthesized AA6061/(TiB_2+Al_2O_3) hybrid aluminium matrix composites". J. Alloys .compo., 2018, 740, 529-535.
22. Zhong, L., Zhao, Y., Zhang, S., Chen, G., Chen, S. and Liu, Y., "Microstructure and mechanical properties of in-situ TiB_2/7055 synthesized by direct magneto chemistry melt reaction". Trans. Non Ferrous. Meter. Soc. China., 2013, 23, 2502-2508.
23. Karantzalis, A. E., Wyatt, S. and Kennady, A. R., "The mechanical properties of Al-TiC metal matrix composites fabricated by a flux –casting technique". Mater. Sci. Engg –A., 1997, 237, 200-206.
24. Siva Prasad, D., Shobha, C. and Ramaiah, N., "Investigations on mechanical properties of aluminium hybrid composites". J. Mater. Res. Technol., 2014, 3, 79-85.
25. Lu, L., Lai, M. O. and Chen, F. L., "Al-4 wt% Cu Composite reinforced with in-situ TiB_2 particles". Acta. Mater., 1997, 45-10, 4297-4309.
26. Lijay, K. J., Selvam, J. D. R., Dinaharan, I. and Vijay. S. J., "Microstructure and mechanical properties characterization of AA6061/TiC aluminium matrix composites synthesized by in situ reaction of silicon carbide and potassium flurotitanate", Trans. Nonferrous Met. Soc. China., 2016, 26, 1791-1800.

[DOI: 10.22068/ijmse.17.1.56]